JOURNAL OF AGRICULTURAL AND FOOD CHEMISTRY

Article

pubs.acs.org/JAFC

Lipase Ligands in *Nelumbo nucifera* Leaves and Study of Their Binding Mechanism

Yuan-Ting Zhu,[†,#] Yan-Wei Jia,[†,#] Yi-Ming Liu,[†,§] Jian Liang,[†] Li-Sheng Ding,[†] and Xun Liao*[,†]

[†]Chengdu Institute of Biology, Chinese Academy of Sciences, Chengdu 610041, China

[§]Department of Chemistry and Biochemistry, Jackson State University, 1400 Lynch Street, Jackson, Mississippi 39217, United States

[#]University of Chinese Academy of Sciences, Beijing 100049, China

ABSTRACT: Lotus (*Nelumbo nucifera*) leaves have been widely used in weight-loss foods to prevent obesity in China. In this work, a facile procedure based on ligand fishing was developed to isolate and identify lipase inhibitors present in lotus leaves. Highly stable and active lipase−Fe_3O_4 superparamagnetic nanoparticle conjugates (LMNPs) were prepared and used as baits. Two flavonoids in lotus leaf extract were found to bind to the baits and were identified as quercetin-3-*O*-*β*-D-arabinopyranosyl-(1→2)- *β*-D-galactopyranoside (**1**) and quercetin-3-*O*-*β*-D-glucuronide (**4**) based on electrospray ionization−mass spectrometric analyses. Their 50% inhibitory concentrations on lipase (IC_{50}) were 52.9 ± 3.2 and 17.1 ± 1.5 *μ*g/mL, respectively. In addition, they were found to significantly quench the fluorescence of lipase, suggesting their strong affinities with this enzyme, which was further evidenced by molecular docking. Ligand fishing based on LMNPs shows great power for fast screening and identification of lipase inhibitors present in edible and medicinal plants.

KEYWORDS: *Nelumbo nucifera leaves, ligand fishing, lipase inhibitors, fluorescence quenching, molecular docking*

INTRODUCTION

Nelumbo nucifera (lotus, belonging to the family of Nelumbonaceae) has long been cultivated in East Asia and extensively used as a traditional medicinal plant as well as health food in China.[1] The leaves are recognized as the medicinal part of *N. nucifera*, as mentioned in the Chinese Pharmacopoeia.[2] The Chinese Food and Drug Administration has approved the use of lotus leaves in both food and drug formulations. For example, they are commonly prepared as weight-loss tea and used in traditional medicines to treat obesity, hyperlipidemia, and hyperglycemia. Flavonoids, alkaloids, and anthocyanins present in lotus leaves are believed to be responsible for a variety of biological effects such as antioxidant, antibacterial, anti-HIV (human immunodeficiency virus), and antiobesity functions.[3−6] In recent years, the antiobesity activity of lotus leaf extract has caught increasing research interest. It was found to be effective in the treatment of obesity induced by high-fat diet in mice,[7] and the total flavonoids in it highly inhibited the activity of porcine pancreatic lipase.[3] However, most of the pharmacological studies focused on the whole extract or the total flavonoids, so little is known about the individual active components in the extract, leaving the molecular basis of the antiobesity effect unclear.

Obesity is caused primarily by lipid metabolism disorder. The enzymes involved in lipid metabolism are usually used as targets in the development of new antiobesity drugs.[8] Pancreatic lipase (PL) is the key enzyme in this process, hydrolyzing 50−70% of total dietary fats.[8] Therefore, lipase inhibitors from plants are considered a good source for antiobesity drugs. In addition, identifying such inhibitors will help to disclose the mechanisms of the plants' nutritious effects.

Activity-guided separation for identifying active ingredients in complex plant extracts usually costs much time and labor. Ligand fishing technology using enzymes immobilized on the surface of solid supports to bind active compounds from a complex matrix based on receptor−ligand affinity adsorption has been developed recently.[9] It has been proven to be an efficient approach for discovering bioactive compounds from extracts of medicinal plants.[10] Magnetic nanoparticles (MNPs) have been used widely as immobilized solid supports due to their excellent convenience in solid−liquid separation. Therefore, ligand fishing based on MNPs can be applied to screen and identify active components from traditional Chinese medicine. We have used human serum albumin, *α*-glucosidase, and protein tyrosine phosphatase 1B-functionalized MNPs for the fast identification of bioactive compounds.[11,12]

Study on the mechanism of molecular interaction between active compounds and enzymes can reveal pharmacokinetics as well as the relationship between the chemical structures and bioactivity of a drug.[13] Fluorescence quenching is a powerful method to investigate the affinity interaction between enzymes and inhibitors and has been widely used for investigating the structure−affinity relationship in binding of drugs to proteins.[14,15] Meanwhile, the molecular modeling study is another important tool for revealing the interactions between enzymes and their inhibitors, which could help to clarify directly the nature of binding between small molecules and enzymes.[16,17]

In this study, a protocol based on ligand fishing for the fast screening and identification of lipase inhibitors from complex matrices such as lotus leaf extract was developed. Highly stable and effective lipase-functionalized MNPs were prepared and evaluated as baits for ligand fishing. HPLC-MS/MS was used to

Received: July 31, 2014
Revised: October 18, 2014
Accepted: October 18, 2014
Published: October 18, 2014

identify the ligands isolated. Moreover, using a fluorescence quenching method and molecular docking, the binding affinity and potential interaction mechanism between the ligands and lipase were investigated.

MATERIALS AND METHODS

Reagents and Chemicals. Dried lotus leaves were obtained from Sichuan province, China. $FeCl_3 \cdot 6H_2O$, $FeCl_2 \cdot 4H_2O$, and *N*,*N*-dimethylformamide (DMF) were purchased from Chengdu Tianhua Chemical Technology Co., Ltd. (Chengdu, China). *N*-Hydroxysuccinimide (NHS), 2-(*N*-morpholino)ethanesulfonic acid (MES), 1-(3-(dimethylamino)propyl)-3-ethylcarbodiimide hydrochloride (EDC·HCl), orlistat, 4-methylumbelliferyl oleate (4-MUO), and porcine pancreatic lipase (type VI-S, from porcine pancreas) were purchased from Sigma Chemical Co. (St. Louis, MO, USA). Tetraethyl orthosilicate (TEOS), succinic anhydride, and 3-aminopropyltrimethoxysilane (APTMS) were purchased from TCI (Tokyo, Japan). The acetonitrile used for HPLC was of chromatographic grade (J. T. Baker, Phillipsburg, NJ, USA). HPLC grade water was produced by a Milli-Q (18.2 MΩ) system (Millipore, Bedford, MA, USA). The other chemicals and solvents were all of analytical reagent grade. Sephadex LH-20 was from Amresco (Solon, OH, USA). D101 macroporous resin, which was a cross-linked polystyrene copolymer, was purchased from the Chemical Plant of Nankai University (Tianjin, China).

Apparatus and Instruments. A TSP HPLC system consisting of quaternary pump and DAD detector (Thermo Separation Products Inc., Waltham, MA, USA) was used for HPLC analysis and ultraviolet (UV) measurement. A Thermo-Quest Finnigan LCQ^{DECA} system equipped with an electrospray ionization source (Thermo-Quest LC/MS Division, USA) was used for HPLC-MS/MS measurements. Fluorescence spectra were recorded by an RF-5301 spectrofluorometer equipped with a 150 W xenon lamp (Shimadzu, Japan). Thermo Scientific Varioskan Flash equipped with a 96-well microplate (Thermo, USA) was used for lipase inhibition assay of active compounds. Ligand fishing was performed in a constant-temperature incubator shaker (Zhengzhou Zhicheng Device Works, Zhengzhou, China). The pH values were measured with a pHS-3 digital pH-meter (Shanghai LeiCi Device Works, Shanghai, China). Preparative separation of active compounds was performed using a Waters 2545 HPLC on a C-18 preparative column (5 μm, 250 × 10 mm i.d.).

Preparation of Lipase-Functionalized MNPs (LMNPs). Lipase-functionalized MNPs were prepared following a previously reported process with a little modification.[18] Briefly, Fe_3O_4 nanoparticles (MNPs) were prepared by coprecipitation of $FeCl_2$ and $FeCl_3$ with ammonia water. Using TEOS and APTMS, the MNPs were first coated with SiO_2, and then the SiO_2 was terminated with amino groups. These amine-terminated MNPs were then treated with 10% succinic anhydride in DMF to obtain carboxyl group-terminated MNPs. Lipase-MNPs coupling was achieved by activating the carboxyl groups with EDC/NHS followed by covalently cross-linking the primary amino groups of the lipase amino acids. LMNPs were suspended in NH_4OAc buffer and stored before use at −4 °C. The immobilized yield of lipase on the MNPs was measured as 50 mg/g MNPs.

Ligand Fishing from Lotus Leaf Extract. Air-dried, powdered lotus leaves (5.0 g) were refluxed with 80% ethanol at 80 °C for 90 min, three times. The extractions were filtered, and all of the filtrates were combined and concentrated to dryness in vacuum at 45 °C to give the crude extract (456.0 mg). The crude extract was suspended in water and fractionated with petroleum ether and ethyl acetate successively. The ethyl acetate fraction was absorbed with a D101 macroporous resin-packed column, washed with water and 30, 50, and 75% alcohol successively. The 50% alcohol eluent was concentrated in vacuum to dryness (named S_0) and used for the following ligand fishing experiment.

Ligand fishing was performed according to the method we reported previously.[11] A 1.0 mg/mL S_0 solution was prepared in ammonium acetate buffer (10 mM, pH 7.4). Twenty milligrams of LMNPs was added to the Eppendorf tube containing 1 mL of S_0 solution. The tube was shaken vigorously for 30 min at 25 °C before being placed on a magnet for 1 min to carry out magnetic liquid−solid separation. The LMNPs were washed three times using 3 × 1 mL buffer to remove nonspecifically bound compounds. Finally, LMNPs were eluted with 1 mL of 50% acetonitrile to release the active compounds. The eluent was stored as solution S_5. S_0 and S_5 were then analyzed with HPLC-MS/MS.

HPLC-DAD-MS/MS Analysis and Compounds Identification. A Tianhe Kromasil C18 column (5 μm, 250 mm × 4.6 mm) kept at 35 °C with a guard column (C18, 5 μm, 4.0 mm × 3.0 mm) was used for chromatographic analysis. The injection volume was 20 μL. The mobile phase was composed of 0.1% HAc (A) and acetonitrile (B), and the column was eluted with a gradient of 10−90% B for 0−50 min at a flow rate of 0.8 mL/min. The peaks were detected by a UV detector set at 280 nm. A Thermo-Quest Finnigan LCQ^{DECA} mass spectrometer equipped with an electrospray ionization source (Thermo-Quest LC/MS Division, USA) was used for HPLC-MS/MS analysis, which gave information on the molecular weights and fragmentation patterns. The mass spectrometry detector parameters were set as follows: nebulizer sheath gas N_2 was 80 units; nebulizer auxiliary gas N_2 was 20 units; capillary temperature was 300 °C; spray voltage was 4.5 kV; capillary voltage was −13 V; and lens voltage was 18 V. All of the data were processed using Finnigan Xcalibur core data system rev. 2.0 (Thermo, USA). Identification of compounds **1**−**6** was realized by comparison of the retention time as well as MS/MS data with those of the known compounds reported previously.[19]

Purification and Identification of the Active Compounds. Five hundred grams of the powdered lotus leaves was extracted and processed according to the method described above. The 50% alcohol eluent fraction was concentrated and redissolved in 50% methanol aqueous solution to submit to Sephadex LH-20 column chromatography eluated with 50% methanol. Elution of fraction A-2 was evaporated under vacuum and recrystallized in methanol to afford compound **1** (15 mg). Elution of fraction B-2 was concentrated and separated by a preparative HPLC system eluated with 40% methanol to give compound **4** (38 mg). Although identified as described above, chemical structures of compound **1** and **4** were further confirmed by comparing the ^1H and ^{13}C NMR data with the published ones. The two isolated compounds were used for subsequent lipase inhibition assay and fluorescence quenching experiment.

Lipase Inhibition Assay. The two bioactive compounds fished out from lotus leaves and the crude extract (S_0) used for ligand fishing process were subjected to lipase inhibition assay with the well-known lipase inhibitor orlistat as positive control.[20] Samples were dissolved in water, whereas both lipase and 4-MUO were dissolved in a buffer containing 13 mM Tris-HCl, 150 mM NaCl, and 1.3 mM $CaCl_2$ (pH 8.0). Briefly, 50 μL of a 0.1 mM 4-MUO solution was mixed with 25 μL of the sample solution into the well of a 96-well microtiter plate, to which 25 μL of the lipase solution (50 U/mL) was added to start the enzymatic reaction. After incubation for 30 min at 25 °C, the enzymatic reaction was stopped by adding 0.1 mL of 0.1 M sodium citrate (pH 4.2). The product of the enzymatic reaction, 4-methylumbelliferone, was quantified with a fluorometric microplate reader (Thermo Scientific Varioskan Flash system) at 355 nm (excitation wavelength) and 460 nm (emission wavelength). All of the assays were performed in triplicate to calculate the mean ± standard deviation values.

Fluorescence Quenching Measurements of Active Compounds with PPL. In the fluorescence quenching experiment, 1.0 μM lipase solution was used. Series concentrations of compounds **1** and **4** (0.013−0.26 mM) were prepared in a buffer of DMSO/H_2O (9:1). Each 0.25 mL of sample solution was added to a 3 mL lipase solution to give a sample concentration in the range of 0.001−0.02 mM. Each mixture was then incubated at 300 K for 0.5 h. The intensity of the fluorescence emission of each mixture at 340 nm was measured at the excitation wavelength of 280 nm, which was repeated three times. Neither compound **1** nor **4** gave out fluorescence emission around 340 nm (in the range of 300−450 nm) at the excitation wavelength. The fluorescence intensities were measured with a Shimadzu RF5301 spectrophotometer with 5.0 nm of excitation and emission slit widths.

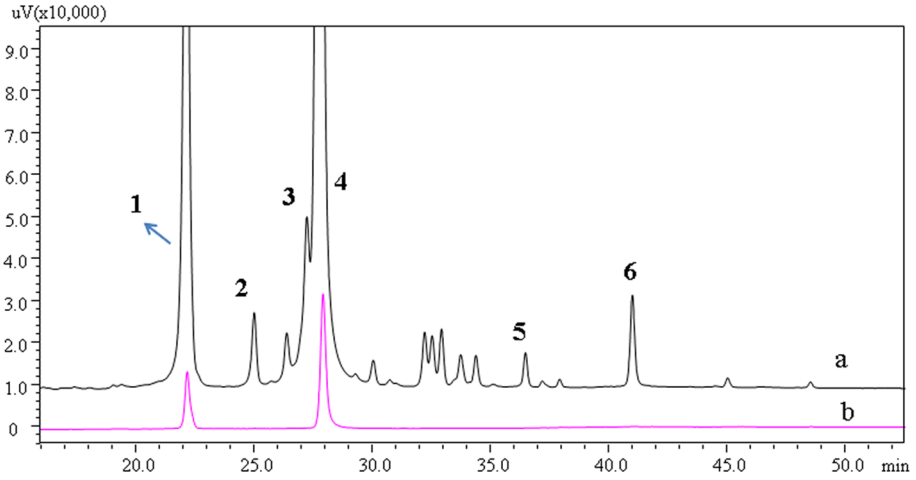

Figure 1. HPLC chromatograms obtained from (a) the extract of lotus leaf (S_0) and (b) the eluent from LMNPs after extraction (S_5). Peaks: 1, quercetin-3-*O*-*β*-D-arabinopyranosyl-(1→2)-*β*-D-galactopyranoside; 2, quercetin-3-*O*-rhamnopyranosyl-(1 → 6)-glucopyranoside; 3, quercetin-3-*O*-glucoside; 4, quercetin-3-*O*-glucuronide; 5, isorhamnetin 3-*O*-*β*-D-xylopyranosyl-(1→2)-*β*-D-glucopyranoside; 6, isorhamnetin 3-*O*-glucoside (**6**).

Table 1. UV−Vis Absorption Maxima (λ_{max}) in HPLC and Main ESI-MS^n Ions of Ingredients in Extracts of Lotus Leaves[a]

compd	identification	t_R (min)	λ_{max} (nm)	NI$^-$	MS/MS
1	quercetin-3-*O*-*β*-D-arabinopyranosyl-(1→2)-*β*-D-galactopyranoside	22.1	227, 254, 354	595	300
2	quercetin-3-*O*-rhamnopyranosyl-(1→6)-glucopyranoside	25.0	227, 254, 354	609	301, 150
3	quercetin-3-*O*-glucoside	27.2	227, 254, 354	463	300
4	quercetin-3-*O*-glucuronide	27.9	229, 254, 354	477	301
5	isorhamnetin 3-*O*-*β*-D-xylopyranosyl-(1→2)-*β*-D-glucopyranoside	36.4	234, 265, 354	609	299, 314
6	isorhamnetin 3-*O*-glucoside	41.0	236, 254, 354	477	314, 299

[a]Compound numbering is in accordance with peak numbering in Figure 1.

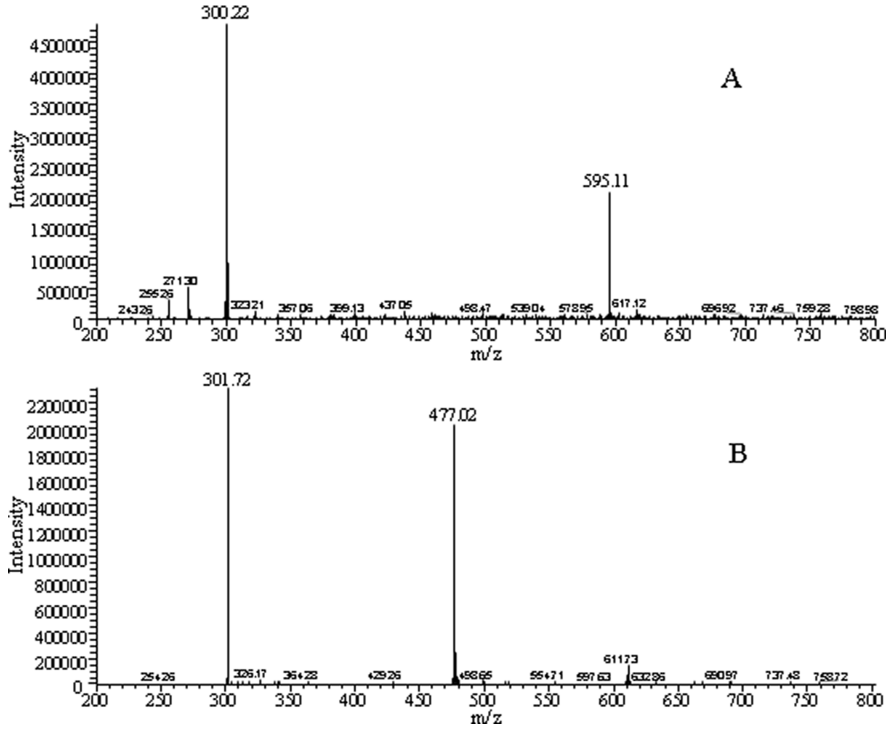

Figure 2. Negative ion CID mass spectra of the two compounds: (A) MS/MS of Qc-3-*O*-AraGal (m/z 595); (B) MS/MS of Qc-3-*O*-Glu (m/z 477).

In addition, synchronous fluorescence spectra of lipase (T = 300 K, pH 7.4) were measured, and the range of synchronous scanning was $\Delta\lambda$ = 60 nm.

The quenching emission data were plotted as a Stern−Volmer plot of F_0/F against [Q], and the quenching constant was calculated by linear regression. Binding constants (K_a) and binding sites (n) were calculated in static quenching by the following equation:

$$\lg[(F_0 - F)/F] = \lg K_a + n \lg[Q] \quad (1)$$

dx.doi.org/10.1021/jf503687e | J. Agric. Food Chem. 2014, 62, 10679−10686

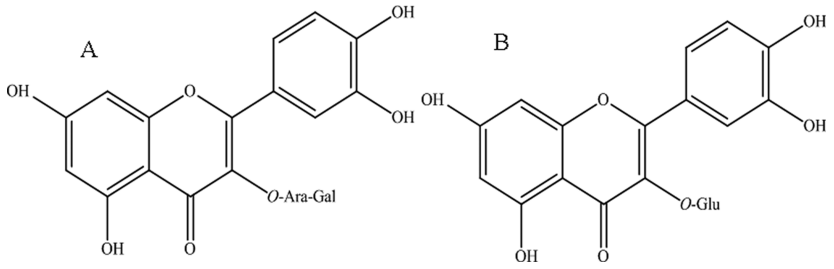

Figure 3. Chemical structures of the ligands isolated from the extract of *Nelumbo nucifera* leaves.

Thermodynamic evaluation of the active compounds with lipase was assessed according to a previously reported method.[20]

Molecular Docking Studies. To investigate the interactions between compounds **1** and **4** with porcine pancreas lipase (PPL), we tried to dock them onto the enzyme. Autodock Vina program was used for in silico molecular docking of the compounds in the active site of lipase.[17] Both compounds were drawn in mol2 format with all hydrogen atoms added, and then the energy was minimized using Hamiltonian-Force-Field-MMFF94x by Molecular Operating Environment (MOE) software. The partial charges were calculated, which were finally saved in pdbqt format. The X-ray crystallographic structure of PPL (Protein Data Bank, PDB entry code 1ETH, 2.80 Å resolution[21]) was downloaded from the Protein Data Bank and opened with Deep View software to check whether the amino acids of the protein were complete or not. Subsequently, all hydrogen atoms and the charges were added for the PPL and also saved as a pdbqt file.

The structure was complexed respectively with the two inhibitors by AutoDock Vina. The catalytic serine residue of the lipase was replaced by glycine residue, and docking runs were subsequently performed to enable the ligand to adopt a suitable position corresponding to the prebound intermediate before the nucleophilic attack in the lipase active site. To fit the active site cleft and allow nonconstructive binding, the appropriate box size for PPL was selected. Using the center of the bound compound, the center of the grid enclosing the box could be defined. The dimensions of the enclosing box were deduced according to the compound size Grid utility program within the Dock 4.0.1 to generate docking grid, which was calculated using box dimensions of 52.65, 45.404, and 123.331. Binding free energies of Qc-3-*O*-AraGal and Qc-3-*O*-Glu were also calculated.

RESULTS AND DISCUSSION

Ligand Fishing from Lotus Leaves Extract with Lipase-Functionalized MNPs. The HPLC chromatograms of lotus leaf extracts before (S_0) and after (S_5) incubation with

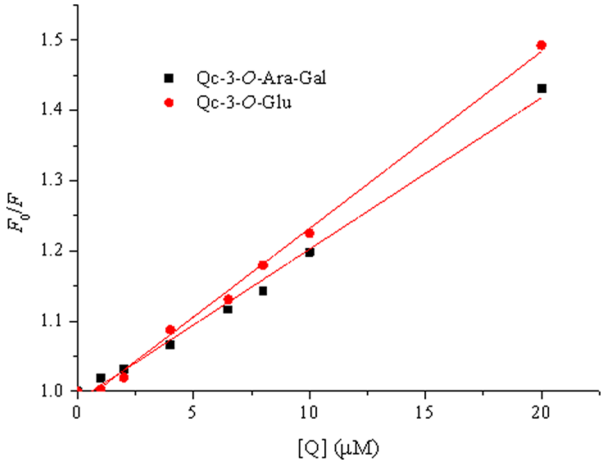

Figure 4. Stern–Volmer plots for the quenching of Qc-3-*O*-AraGal and Qc-3-*O*-Glu on the PPL at 300 K.

Table 2. Stern–Volmer Quenching Constants for the Interaction of Qc-3-*O*-AraGal and Qc-3-*O*-Glu with PPL at 300 K

compd	temp (K)	$K_{SV}/10^4$ (L mol^{-1})	$k_q/10^{12}$ (L mol^{-1} s^{-1})	R^2
Qc-3-*O*-AraGal	300	2.157	2.157	0.992
Qc-3-*O*-Glu	300	2.521	2.521	0.995

Table 3. Relative Thermodynamic Parameters of the Interaction of Active Compounds with PPL

compd	temp (K)	ΔG (kJ mol^{-1})	ΔH (kJ mol^{-1})	ΔS (J mol^{-1} K^{-1})
Qc-3-*O*-AraGal	300	−24.890	3.091	93.270
Qc-3-*O*-Glu	300	−25.278	9.782	116.867

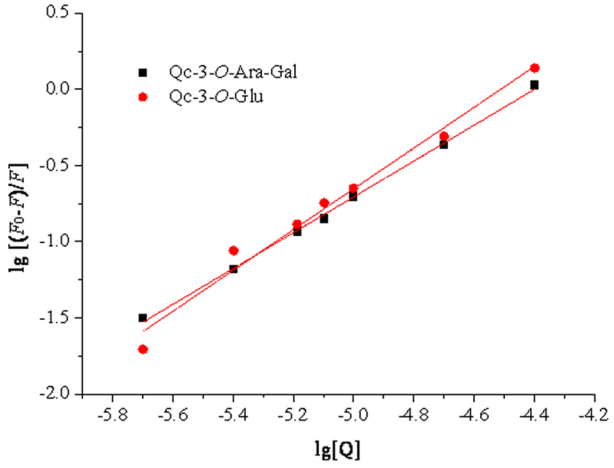

Figure 5. Plots of lg$[(F_0 - F)/F]$ versus lg[Q] for Qc-3-*O*-AraGal and Qc-3-*O*-Glu at 300 K.

Table 4. Binding Constant K_a and the Number of Binding Sites (n) at Different Temperatures

compd	temp (K)	$K_a/10^5$ (L mol^{-1})	n	R^2
Qc-3-*O*-AraGal	300	1.491	1.176	0.998
Qc-3-*O*-Glu	300	10.926	1.338	0.979

LMNPs are shown in Figure 1. As in Figure 1a, the crude extracts (S_0) from lotus leaves possessed a complicated composition containing a variety of flavonoid compounds. The chromatographic and MS data of the main flavonoids from S_0 are listed in Table 1. By comparison of HPLC retention time, molecular weight, and MS/MS data with those reported in the literature previously,[19] six flavonoids were identified as quercetin-3-*O*-*β*-D-arabinopyranosyl-(1→2)-*β*-D-galactopyranoside (**1**), quercetin-3-*O*-rhamnopyranosyl-(1→6)-glucopyrano-

dx.doi.org/10.1021/jf503687e | J. Agric. Food Chem. 2014, 62, 10679−10686

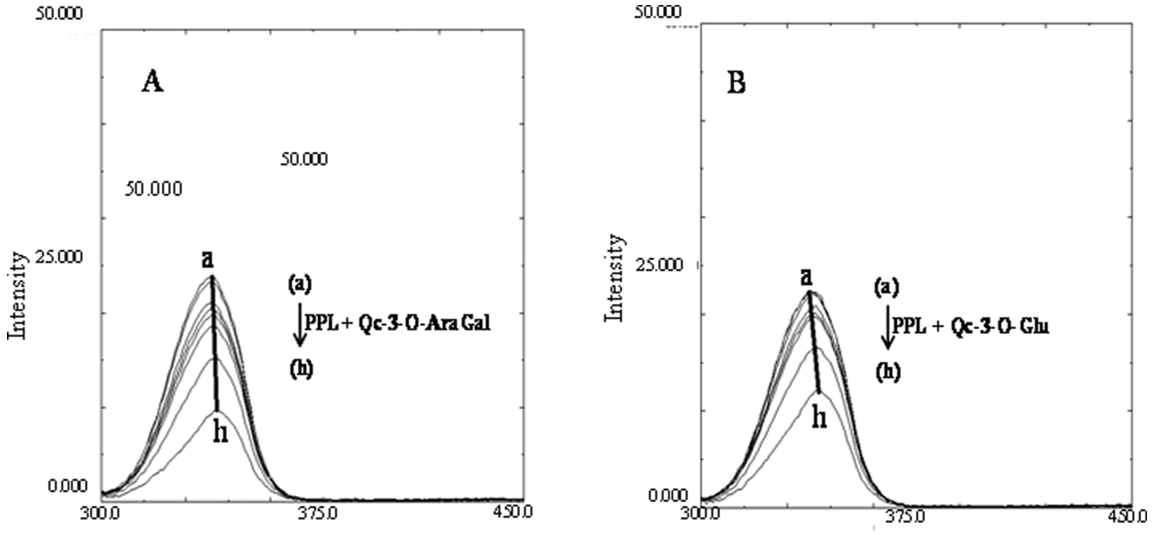

Figure 6. Synchronous fluorescence spectra of PPL at various concentrations of Qc-3-*O*-AraGal (A) and Qc-3-*O*-Glu (B) at 60 nm wavelength interval, T = 310 K, c(PPL) = 1.0×10^{-6} mol L^{-1}; c(Qc-3-*O*-AraGal), and c(Qc-3-*O*-Glu)/(10^{-6} mol L^{-1}) a–h: 0, 1, 2, 4, 6.5, 8, 10, 20, respectively.

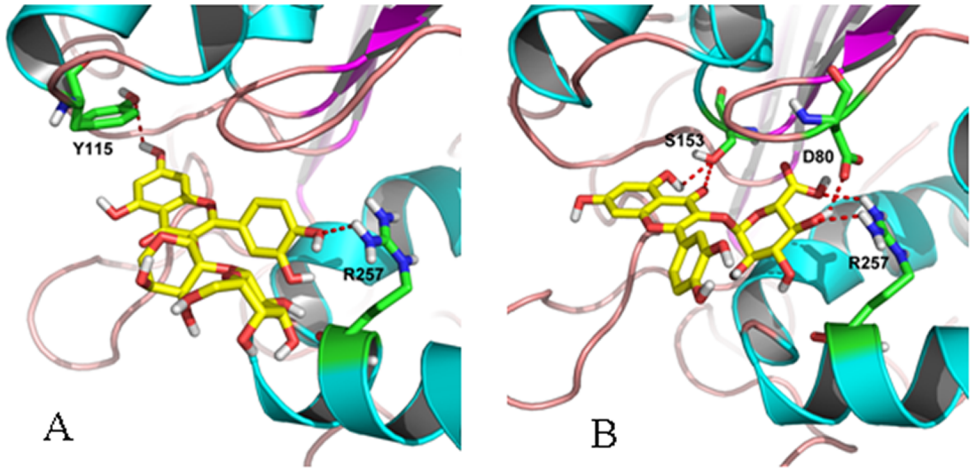

Figure 7. Superimposition of the top-scoring docking positions of (A) Qc-3-*O*-AraGal and (B) Qc-3-*O*-Glu in PPL active sites. Each inhibitor is represented in atom color-code sticks (oxygen, red). Structures were drawn with PyMOL Molecular Graphics System (version 1.3, Schrodinger, LLC), using the following PDB file: 1ETH for PPL.

side (**2**), quercetin-3-*O*-glucoside (**3**), quercetin-3-*O*-glucuronide (**4**), isorhamnetin 3-*O*-*β*-D-xylopyranosyl-(1→2)- *β*-D-glucopyranoside (**5**), and isorhamnetin 3-*O*-glucoside (**6**). Two compounds (**1** and **4**) were found in S_5 as shown in Figure 1b, indicating that there were only two lipase ligands in the lotus leaf crude extracts which can bind to LMNPs. They were isolated from the extracts for subsequent lipase inhibition assay and fluorescence quenching experiment, and their chemical structures were confirmed as following.

The UV absorption maximum (λ_{max}, nm) of both **1** and **4** were at ∼254 nm (Figure 2), which were consistent with those of quercetin type flavonoids.[22] Compound **1** has a molecular weight of 596 (m/z 595, $[M - H]^-$). The radical aglycone ion at m/z 300 $[A - 2H]^-$ in MS^2 (Figure 2A) indicated that the interglycosidic linkage between the two monosaccharides was C1→C2.[22] Therefore, this compound was identified as quercetin-3-*O*-*β*-D-arabinopyranosyl-(1→2)-*β*-D-galactopyranoside (Qc-3-*O*-AraGal). Compound **2** was found to have a molecular weight of 478 (m/z 477, $[M - H]^-$). A significantly strong aglycone ion peak was observed at m/z 301 $[A - H]^-$ in MS^2 (Figure 2B), indicating that it was a glucuronic acid glycoside. Therefore, compound **2** was identified as quercetin 3-*O*-D-glucuronide (Qc-3-*O*-Glu), which was the dominant flavonoid in lotus leaves.[19] Their chemical structures are shown in Figure 3.

It is worth noting that only two flavonoids (compounds **1** and **4**) were fished out from the mixture of many flavonoids present in the extract, and only these two exhibited potent binding ability to PPL. As all six identified flavonoids have the same aglycones, that is, quercetin or isorhamnetin, we speculated that it was the complicated conformation of the different sugar chains that caused such difference in lipase binding. This result corresponds largely to a previous study in which lipase immobilized on hollow fiber was used to select lipase inhibitors from lotus leaf.[23] The only difference is that, apart from compounds **1** and **4**, another kaempferol type flavonoid was extracted in the study. However, it showed significantly lower bioactivity and binding capacity compared with compounds **1** and **4**.

Lipase Inhibition Assay. The beneficial effects of lotus leaves have been mainly attributed to their high flavonoid contents. To our knowledge, this is the first screening of lipase

inhibitors from lotus leaves by LMNP-based ligand fishing. The PPL inhibitory activities of the two PPL-bound flavonoids, Qc-3-*O*-AraGal (**1**) and Qc-3-*O*-Glu (**2**), together with the crude extract of lotus leaves (S_0) were evaluated by a traditional PL inhibitor assay[20] with orlistat as the positive control. The lipase inhibitory activities of the samples were determined using 4-MUO as the substrate of the lipase-catalyzing reaction. They were determined by measuring the fluorescence intensity increment arising from the fluorescent product 4-methylumbelliferone (4-MU) at an excitation wavelength of 360 nm and an emission wavelength of 450 nm using a 96-well microplate reader. Compared to the IC_{50} value of orlistat (1.53 ± 0.02 μM), those for compounds **1**, **4**, and S_0 were 52.9 ± 3.2 μg/mL (88.8 ± 5.4 μM), 17.1 ± 1.5 μg/mL (35.8 ± 3.1 μM), and 95.0 ± 5.1 μg/mL, respectively. The two active compounds (**1** and **4**) showed significantly stronger inhibitory effects than the crude extracts (S_0). These results indicate that both compounds fished out by this method are effective inhibitors of lipase. This finding is in agreement with a previous report.[24] Therefore, this method is expected to be useful for activity-guided separation of active compounds from natural products.

Fluorescence Quenching Measurements of Active Compounds with PPL. *Fluorescence Quenching Mechanism.* The intrinsic fluorescence is usually used to investigate the structure and dynamics of proteins; therefore, it is a good tool in the study of association reactions between proteins and bioactive compounds.[24] When the excitation wavelength was set at 280 nm, the fluorescence emission peaks of PPL (at 340 nm) mixed with a series concentrations of the quencher provided information on tryptophan residues, which are the main contributors to intrinsic fluorescence of proteins.[25] Fluorescence quenching can thus be used to measure binding affinity. Fluorescence quenching is described by the Stern−Volmer equation as follows:

$$\frac{F_0}{F} = 1 + k_q\tau_0[Q] = 1 + K_{SV}[Q] \quad (2)$$

F_0 and F are the fluorescence intensity before and after quencher was added to PPL; k_q is the quenching rate constant, K_{SV} is the Stern−Volmer dynamic quenching constant, τ_0 is the average lifetime of bimolecular fluorescence without quencher ($\tau_0 = 10^{-8}$ s), and [Q] is the concentration of the quencher. K_{SV} was determined by linear regression of a plot of F_0/F against [Q], and it is the slop of linear regression of eq 2. In this work, Stern−Volmer plots for PPL fluorescence quenching by Qc-3-*O*-AraGal and Qc-3-*O*-Glu are shown in Figure 4, and K_{SV} and k_q at pH 7.4 are summarized in Table 2. A linear Stern−Volmer plot usually indicates a single way of quenching, in which the fluorophores are all equally accessible to the quencher. On the other hand, when the fluorophores are quenched by both collision and complex formation with the quencher, the Stern−Volmer plot will exhibit an upward curvature, corresponding to the occurrence of both dynamic and static quenching. In this work, the plots of the two flavonoids were in good agreement with the linear Stern−Volmer plot, whereas no obvious deviation toward the *y*-axis was observed, indicating that either dynamic quenching or static quenching was predominant.[26]

The k_q value reflects the efficiency of quenching or the accessibility of the fluorophores to the quencher and, thus, is used to judge whether the formation of a complex can lead to the quenching.[27]The k_q value near 1×10^{10} M^{-1} s^{-1} is typical for dynamic quenching mechanism. In this work, the k_q values of Qc-3-*O*-AraGal and Qc-3-*O*-Glu were 200-fold (2.157×10^{12} L mol^{-1} s^{-1}) and 250-fold (2.521×10^{12} L mol^{-1} s^{-1}) higher than 1×10^{10} M^{-1} s^{-1}, respectively. This result suggested that both compounds formed a complex with PPL and both belonged to static quenching mechanism. Moreover, Qc-3-*O*-Glu showed higher fluorescence quenching effects on PPL than Qc-3-*O*-AraGal.

Thermodynamic Parameters and the Characteristic of the Binding Forces. The binding of ligands to proteins is mainly affected by noncovalent interactions including hydrogen bonds, van der Waals forces, electrostatic interactions, and hydrophobic interactions. These acting forces can be confirmed by thermodynamic parameters of the binding reaction. Therefore, the interaction of the two flavonoids with PPL identified by thermodynamic parameters dependent on temperature are calculated from van't Hoff equations:

$$\ln(K_2/K_1) = \left(\frac{1}{T_1} - \frac{1}{T_2}\right)\Delta H/R \quad (3)$$

$$\Delta G = \Delta H - T\Delta S = -RT\ln K \quad (4)$$

where T is the experimental temperature, ΔH is the enthalpy change, R is the gas constant, ΔS is the entropy change, K_2 and K_1 are the binding constants (K_a) at the corresponding T, and ΔG is the free energy change.

The values of ΔH, ΔS, and ΔG obtained are shown in Table 3. The negative value for ΔG indicated a spontaneous interaction process. For both Qc-3-*O*-AraGal (+93.270 J mol^{-1} K^{-1}) and Qc-3-*O*-Glu (+116.867 J mol^{-1} K^{-1}), from the point of water structure, the positive ΔS values reflected a hydrophobic interaction.[28] In particular, the specific positive ΔH and ΔS values indicated that hydrophobic interaction was the major acting force and the reaction was mainly driven by entropy. These interactions could proceed through aromatic rings and other hydrophobic groups of the two active compounds. In addition to hydrophobic forces, hydrogen bonding between OH groups and the side chain of amino acids was also involved in the interaction of the two active compounds with PPL at the molecular level.

Numbers of Binding Sites (n) and Binding Constants (K_a). For static quenching, the binding sites and constants were calculated according to the following double-logarithm equation:[29]

$$\lg\frac{F_0 - F}{F} = \lg K_a + n\lg[Q] \quad (1)$$

F_0 and F are the fluorescence intensities of PPL in the absence and presence of both compounds; K_a is the binding constant; n is the number of binding sites; and [Q] is the concentration of the quencher. The dependence of $\lg[(F_0 - F)/F]$ on $\lg[Q]$ value was linear, the slope of which equals n, and intercept to $\lg[K_a]$. Plots of $\lg[(F_0 - F)/F]$ versus $\lg[Q]$ for Qc-3-*O*-AraGal and Qc-3-*O*-Glu to PPL are shown in Figure 5. The double-logarithm curves for both active compounds were obviously linear. The corresponding calculated K_a (n) values between Qc-3-*O*-AraGal or Qc-3-*O*-Glu and PPL were 1.491×10^5 (1.176) and 10.926×10^5 (1.338) at 300 K, respectively. The active compound Qc-3-*O*-Glu showed an obviously stronger binding capacity than Qc-3-*O*-AraGal (Table 4).

Characteristics of Synchronous Fluorescence Spectra. To investigate the effect of active compounds on the structural change of PPL, synchronous fluorescence spectra of PPL with different concentrations of active compounds were measured by simultaneously scanning the excitation and emission mono-

chromators. Qc-3-O-AraGal and Qc-3-O-Glu were measured individually under the same condition to exclude the possible interruption. Because none of them showed signals, no background control was needed in the following experiment. The synchronous fluorescence spectra have advantages of reducing bandwidth and avoiding various perturbations. It shows only the characteristics of tyrosine and tryptophan residues of PPL under wavelength interval ($\Delta\lambda$) between 15 and 60 nm, respectively. The maximum excitation and emission wavelengths of the residues correlate to the polarity of the microenvironment and, thus, can be used to judge the conformational change of proteins.

The effect of the two active compounds on PPL synchronous fluorescence spectroscopy is shown in Figure 6. The emission maximum of tryptophan residues exhibited a significant red shift (from 338 to 342 nm) for both Qc-3-O-AraGal and Qc-3-Glu, indicating an increase of polarity around the tryptophan residues and a decrease of the hydrophobicity. The results showed the conformational change of PPL tryptophan microregion by addition of active compounds during the binding process.

Molecular Docking. In silico molecular docking provided additional explanation for the experimental inhibition activity of Qc-3-*O*-AraGal and Qc-3-*O*-Glu. The porcine pancreatic lipase possesses two domains. Its N-terminal domain is an α/β hydrolase fold, which contains the catalytic sites of Ser153, Asp177, and His264. The crystal structure of the ternary porcine lipase-colipase-tetraethylene glycol monooctyl ether showed that the overall position of the three catalytic sites is conservative in different species.[21] The crystal structure of PPL (1ETH) was determined at a resolution of 2.80 Å, and the lipase active site was fully accessible so that docking experiments with the two inhibitors could be carried out. The in silico docking experiment showed that Qc-3-*O*-AraGal mostly interacted with PPL through hydrogen bonding of Tyr115 with the 7-hydroxyl group on ring A and Arg257 with the 3′-hyroxyl group on ring B (Figure 7A). Docking of Qc-3-*O*-Glu to PPL also showed an apparent hydrogen-bonding network resulting from the interaction of the 5-hyrdoxyl group on ring A and carbonyl group on ring C with the PPL catalytic residue Ser153. Additionally, the carboxyl and hydroxyl moieties on the sugar residue together had strong hydrogen-bonding interactions with the side chain of the PPL catalytic residue Arg257; the hydroxyl group on the sugar residue also showed hydrogen-bonding interaction with PPL residue Asp80 (Figure 7B). The estimated binding energies were −9.2 kcal mol^{-1} for Qc-3-*O*-Glu and −7.9 kcal mol^{-1} for Qc-3-*O*-AraGal, respectively. The docking results suggested that the two compounds from the screen might be potential inhibitors of PPL. In addition, the different binding free energies of Qc-3-*O*-Glu and Qc-3-*O*-AraGal suggested that Qc-3-*O*-Glu had a higher affinity than Qc-3-*O*-AraGal for PPL, which was consistent with the results of the lipase inhibition assay in vitro and fluorescence quenching analysis.

In conclusion, an effective method based on ligand fishing was developed to screen lipase inhibitors from complex chemical mixtures. Pancreatic porcine lipase immobilized onto magnetic nanoparticles was used to bind the ligands from the complex mixtures, and then the bound ligands could be easily separated magnetically for HPLC-MS/MS analysis. This method was first employed in lotus leaf extract to identify two flavonoids that showed significant inhibitory effect toward lipase, and the mechanism of PPL inhibition of the two ligands was investigated by fluorescence quenching together with molecular docking. The result of this study adds to the understanding of the mechanism of health effects of lotus leaves, and the method proposed shows great potential in screening enzyme inhibitors from edible and medicinal plants.

AUTHOR INFORMATION

Corresponding Author

*(X.L.) Phone/fax: +86 28 82890402. E-mail: liaoxun@cib.ac.cn.

Funding

We appreciate the financial support from the National Natural Science Foundation of China (81173536 and 21072184 to X.L.) and the U.S. National Institutes of Health (GM 089557 to Y.-M.L.).

Notes

The authors declare no competing financial interest.

ABBREVIATIONS USED

MNPs, magnetic nanoparticles; Qc-3-*O*-AraGal, quercetin-3-*O*-β-D-arabinopyranosyl-(1→2)-β-D-galactopyranoside; Qc-3-*O*-Glu, quercetin-3-*O*-β-D-glucuronide; IC_{50}, 50% inhibitory concentration; 4-MUO, 4-methylumbelliferyl oleate; 4-MU, 4-methylumbelliferone; PPL, porcine pancreas lipase; LMNPs, lipase-functionalized MNPs; NI^-, negative ion mode

REFERENCES

(1) Tang, W.; Eisenbrand, G. *Nelumbo nucifera* Gaertn. In *Chinese Drugs of Plant Origin*; Springer: Berlin, Germany, 1992; pp 697−701.

(2) Guo, H. Cultivation of lotus (*Nelumbo nucifera* Gaertn. ssp. *nucifera*) and its utilization in China. *Genet. Resour. Crop Evol.* **2009**, *56*, 323−330.

(3) Liu, S.; Li, D.; Huang, B.; Chen, Y.; Lu, X.; Wang, Y. Inhibition of pancreatic lipase, α-glucosidase, α-amylase, and hypolipidemic effects of the total flavonoids from *Nelumbo nucifera* leaves. *J. Ethnopharmacol.* **2013**, *149*, 263−269.

(4) Tho Chau Minh Vinh, D.; Tuan Duc, N.; Hung, T.; Stuppner, H.; Ganzera, M. Analysis of alkaloids in lotus (*Nelumbo nucifera* Gaertn.) leaves by non-aqueous capillary electrophoresis using ultraviolet and mass spectrometric detection. *J. Chromatogr., A* **2013**, *1302*, 174−180.

(5) Mukherjee, P. K.; Mukherjee, D.; Maji, A. K.; Rai, S.; Heinrich, M. The sacred lotus (*Nelumbo nucifera*) − phytochemical and therapeutic profile. *J. Pharm. Pharmacol.* **2009**, *61*, 407−422.

(6) Li, M.; Xu, Z. Quercetin in a lotus leaves extract may be responsible for antibacterial activity. *Arch. Pharmacal Res.* **2008**, *31*, 640−644.

(7) Ono, Y.; Hattori, E.; Fukaya, Y.; Imai, S.; Ohizumi, Y. Anti-obesity effect of *Nelumbo nucifera* leaves extract in mice and rats. *J. Ethnopharmacol.* **2006**, *106*, 238−244.

(8) Birari, R. B.; Bhutani, K. K. Pancreatic lipase inhibitors from natural sources: unexplored potential. *Drug Discovery Today* **2007**, *12*, 879−889.

(9) Moaddel, R.; Marszall, M.; Bighi, F.; Yang, Q.; Duan, X.; Wainer, I. Automated ligand fishing using human serum albumin-coated magnetic beads. *Anal. Chem.* **2007**, *79*, 5414−5417.

(10) Yasuda, M.; Wilson, D.; Fugmann, S.; Moaddel, R. Synthesis and characterization of SIRT6 protein coated magnetic beads: Identification of a novel inhibitor of SIRT6 deacetylase from medicinal plant extracts. *Anal. Chem.* **2011**, *83*, 7400−7407.

(11) Qing, L.-S.; Xue, Y.; Zheng, Y.; Xiong, J.; Liao, X.; Ding, L.-S.; Li, B.-G.; Liu, Y.-M. Ligand fishing from *Dioscorea nipponica* extract using human serum albumin functionalized magnetic nanoparticles. *J. Chromatogr., A* **2010**, *1217*, 4663−4668.

(12) Qing, L. S.; Tang, N.; Xue, Y.; Liang, J.; Liu, Y. M.; Liao, X. Identification of enzyme inhibitors using therapeutic target protein−magnetic nanoparticle conjugates. *Anal. Methods* **2012**, *4*, 1612−1615.
(13) Yanagisawa, M.; Sugiya, M.; Iijima, H.; Nakagome, I.; Hirono, S.; Tsuda, T. Genistein and daidzein, typical soy isoflavones, inhibit TNF-α-mediated downregulation of adiponectin expression via different mechanisms in 3T3-L1 adipocytes. *Mol. Nutr. Food. Res.* **2012**, *56*, 1783−1793.
(14) Wang, Y. Q.; Zhang, H. M.; Zhang, G. C.; Tao, W.-H.; Tang, S.-H. Binding of brucine to human serum albumin. *J. Mol. Struct.* **2007**, *830*, 40−45.
(15) Li, Y. Q.; Zhou, F. C.; Gao, F.; Bian, J. S.; Shan, F. Comparative evaluation of quercetin, isoquercetin and rutin as inhibitors of α-glucosidase. *J. Agric. Food Chem.* **2009**, *57*, 11463−11468.
(16) Park, H.; Hwang, K. Y.; Oh, K. H.; Kim, Y. H.; Lee, J. Y.; Kim, K. Discovery of novel α-glucosidase inhibitors based on the virtual screening with the homology-modeled protein structure. *Bioorg. Med. Chem.* **2008**, *16*, 284−292.
(17) Point, V.; Kumar, K. V. P. P.; Marc, S.; Delorme, V.; Parsiegla, G.; Amara, S.; Carriere, F.; Buono, G.; Fotiadu, F.; Canaan, S.; Leclaire, J.; Cavalier, J.-F. Analysis of the discriminative inhibition of mammalian digestive lipases by 3-phenyl substituted 1,3,4-oxadiazol-2(3*H*)-ones. *Eur. J. Med. Chem.* **2012**, *58*, 452−463.
(18) Qing, L. S.; Xiong, J.; Xue, Y.; Liu, Y. M.; Guang, B.; Ding, L. S.; Liao, X. Using baicalin-functionalized magnetic nanoparticles for selectively extracting flavonoids from *Rosa chinensis*. *J. Sep. Sci.* **2011**, *34*, 3240−3245.
(19) Chen, S.; Wu, B. H.; Fang, J. B.; Liu, Y. L.; Zhang, H. H.; Fang, L. C.; Guan, L.; Li, S. H. Analysis of flavonoids from lotus (*Nelumbo nucifera*) leaves using high performance liquid chromatography/photodiode array detector tandem electrospray ionization mass spectrometry and an extraction method optimized by orthogonal design. *J. Chromatogr., A* **2012**, *1227*, 145−153.
(20) Nakai, M.; Fukui, Y.; Asami, S.; Toyoda-Ono, Y.; Iwashita, T.; Shibata, H.; Mitsunaga, T.; Hashimoto, F.; Kiso, Y. Inhibitory effects of oolong tea polyphenols on pancreatic lipase in vitro. *J. Agric. Food Chem.* **2005**, *53*, 4593−4598.
(21) Hermoso, J.; Pignol, D.; Kerfelec, B.; Crenon, I.; Chapus, C.; FontecillaCamps, J. C. Lipase activation by nonionic detergents − the crystal structure of the porcine lipase-colipase-tetraethylene glycol monooctyl ether complex. *J. Biol. Chem.* **1996**, *271*, 18007−18016.
(22) Qing, L. S.; Xue, Y.; Zhang, J. G.; Zhang, Z. F.; Liang, J.; Jiang, Y.; Liu, Y.-M.; Liao, X. Identification of flavonoid glycosides in *Rosa chinensis* flowers by liquid chromatography−tandem mass spectrometry in combination with ^{13}C nuclear magnetic resonance. *J. Chromatogr., A* **2012**, *1249*, 130−137.
(23) Tao, Y.; Zhang, Y.; Wang, Y.; Cheng, Y. Hollow fiber based affinity selection combined with high performance liquid chromatography-mass spectroscopy for rapid screening lipase inhibitors from lotus leaf. *Anal. Chim. Acta* **2013**, *785*, 75−81.
(24) Wang, Y.-Q.; Zhang, H.-M.; Zhang, G.-C.; Tao, W.-H.; Tang, S.-H. Interaction of the flavonoid hesperidin with bovine serum albumin: a fluorescence quenching study. *J. Lumin.* **2007**, *126*, 211−218.
(25) Ladokhin, A. S. Fluorescence spectroscopy in peptide and protein analysis. In *Encyclopedia of Analytical Chemistry*; Wiley: New York, 2000; pp 5762−5769.
(26) Soares, S.; Mateus, N.; De Freitas, V. Interaction of different polyphenols with bovine serum albumin (BSA) and human salivary α-amylase (HSA) by fluorescence quenching. *J. Agric. Food Chem.* **2007**, *55*, 6726−6735.
(27) Eftink, M. R. Fluorescence quenching reactions. In *Biophysical and Biochemical Aspects of Fluorescence Spectroscopy*; Springer: Berlin, Germany, 1991; pp 1−41.
(28) Daneshgar, P.; Moosavi-Movahedi, A. A.; Norouzi, P.; Ganjali, M. R.; Madadkar-Sobhani, A.; Saboury, A. A. Molecular interaction of human serum albumin with paracetamol: spectroscopic and molecular modeling studies. *Int. J. Biol. Macromol.* **2009**, *45*, 129−134.
(29) Wang, Y. P.; Wei, Y. L.; Dong, C. Study on the interaction of 3,3-bis(4-hydroxy-1-naphthyl)-phthalide with bovine serum albumin by fluorescence spectroscopy. *J. Photochem. Photobiol. A* **2006**, *177*, 6−11.